Preparation of ZIF-8 particles via solvent thermal synthesis and investigation of their photocatalytic hydrogen generation performance

Chong Lin[1], Changhui Xiao[2], Dongyang Zhang[3], Houdong Rao[4], Wei Cheng[5]
Luoyang Ship Material Research Institute, Luoyang, 471023, China
[4]Corresponding author
E-mail: [1]*lc725s@163.com*, [2]*xiaochanghui725@126.com*, [3]*zdy_dut@163.com*, [4]*838020036@qq.com*, [5]*chengwei@725.com.cn*

Received 21 September 2023; accepted 9 October 2023; published online 27 November 2023
DOI https://doi.org/10.21595/vp.2023.23648

67th International Conference on Vibroengineering in Udaipur, India, November 27, 2023

Abstract. In recent years, the preparation and application of ZIF-8 nanoparticles have garnered interest, yet systematic studies on the relationship between their size and photocatalytic hydrogen generation performance remain limited. Addressing this gap, the present study pioneers an in-depth exploration of the preparation of ZIF-8 nanoparticles, emphasizing their impact on photocatalytic hydrogen generation. A novel observation was made, where uniform ZIF-8 particles of approximately 1 micron were optimally synthesized at a molar ratio of zinc acetate to dimethylimidazole of 1:4. Interestingly, the study unveiled a unique trend of ZIF-8 particle size variation with changing reaction temperatures. Most notably, and for the first time, this research underscores the paramount role of particle size on ZIF-8's hydrogen generation capability, connecting it intricately to the material's pore characteristics. An unprecedented finding was the superior performance of the 500 nanometer-sized ZIF-8 in photocatalytic hydrogen generation, attributing its excellence to its pore size being finely attuned to the photocatalytic reaction requirements. Such groundbreaking insights not only deepen our comprehension of ZIF-8 materials but also hold transformative potential for the international engineering community, particularly in tailoring applications for enhanced photocatalytic hydrogen generation.

Keywords: solvent-thermal synthesis, zif-8, particle size, photocatalytic hydrogen production.

1. Introduction

Metal-organic frameworks (MOFs), a class of materials with highly ordered porous structures, have attracted widespread attention in recent years. The pore structures and abundant active sites of MOF materials endow them with potential applications in areas such as gas storage, separation, and catalysis [1-3]. Among these, Zeolitic Imidazolate Framework-8 (ZIF-8), as an important type of MOF material, possesses unique crystal structures and porous properties, making it a notable candidate in the field of catalysis. ZIF-8's compositional diversity and tunable structure render it a promising material for photocatalytic hydrogen production [4-6].

However, despite the considerable potential of ZIF-8 in photocatalytic hydrogen production, its performance is influenced by various factors, including particle size and structure. Particle size plays a crucial role in the photocatalytic performance of MOF materials. On one hand, changes in particle size can alter the material's light absorption and transmission properties, thereby affecting the progress of photocatalytic reactions. On the other hand, particle size also impacts the size and distribution of material pores, subsequently affecting the exposure level of catalytic active sites. Therefore, in-depth investigation into the influence of particle size on the photocatalytic hydrogen production performance of ZIF-8 is of significant importance [7].

Building on this foundation, our research stands as a pioneering endeavor, meticulously probing into the realm of ZIF-8 nanoparticles, delving deep into their synthesis, and their subsequent application in photocatalytic hydrogen production. Specifically, we first explore the

mechanism of controlling ZIF-8 particle size through the adjustment of reactant ratios. Subsequently, we study ZIF-8 prepared at different reaction temperatures to gain deeper insights into the influence of temperature factors on particle size. Lastly, we examine the performance of ZIF-8 particles of different sizes in the photocatalytic hydrogen production reaction to reveal the mechanisms through which particle size affects photocatalytic performance.

The ambition of our study surpasses merely understanding the synthesis and performance of ZIF-8 nanoparticles. We are at the frontier of providing a rigorous scientific foundation for the potential of ZIF-8 in the realm of photocatalytic hydrogen production. By expertly manipulating pivotal factors such as reactant ratios and temperature, we not only engineer ZIF-8 nanoparticles of diverse sizes but also demystify the performance trends in photocatalytic hydrogen production. This work, thus, unveils previously concealed facets of the photocatalytic hydrogen production mechanism inherent to ZIF-8 materials. By charting this novel territory in MOF materials for photocatalysis, our research stands as a beacon, heralding innovative pathways for the evolution of clean energy technologies.

2. Experiment

2.1. Experimental materials and equipment

Dimethylimidazole, anhydrous methanol, China National Pharmaceutical Group Chemical Reagent Co., Ltd.; Zinc acetate, Belun Technology Co., Ltd.

AB204-E Analytical Balance, S312-90 Constant Speed Stirrer, C-MAG HS7 digital Heating Magnetic Stirrer, KQ5200DE CNC Ultrasonic Cleaner, AXTG16G Benchtop General-purpose Centrifuge.

2.2. Preparation of ZIF-8 particles

First, prepare solution A by dissolving the predetermined amount of zinc acetate in 100 milliliters of methanol. Simultaneously, prepare solution B containing the predetermined amount of dimethylimidazole, also added to 100 milliliters of methanol solvent. Next, slowly pour solution B into solution A while maintaining continuous heating and stirring for 2 hours. Within these 2 hours, ensure that the reaction occurs and that the mixture reacts fully through heating and stirring. Subsequently, use centrifugal separation to isolate the reaction product from the solution. For the separated product, perform multiple washes with methanol to remove possible impurities and byproducts. The focus of this experiment is to investigate the effect of different molar ratios of reactants zinc acetate and dimethylimidazole on particle size. Specifically, three molar ratios, 1:2, 1:4, and 1:8, were examined, with the 1:4 ratio chosen as the baseline. Additionally, the experiment examined different reaction temperatures, including 30 °C, 40 °C, 50 °C, and 60 °C.

2.3. Characterization of photocatalytic properties

Firstly, take 10 milligrams of catalyst and disperse it in 20 milliliters of aqueous solution. To enhance the efficiency of the catalytic reaction, add 5 milliliters of triethanolamine as a sacrificial agent in the system. Disperse the catalyst uniformly in the solution through ultrasonic treatment, which helps increase the catalyst's surface area and thus enhances the reaction efficiency. The ultrasonic treatment continues for 10 minutes to ensure even dispersion of the catalyst. Then, seal the reaction system to prevent gas escape and gradually introduce a 30-minute flow of argon gas to purge oxygen and other impurity gases from the system.

Subsequently, under appropriate stirring conditions, start the CEL-HXF300 xenon lamp to provide full-spectrum illumination. Samples from the reaction system are collected every 1 hour. The collected samples are then introduced into the thermal conductivity detector (TCD) channel of the gas chromatograph (GC9800) equipped with a 5 A molecular sieve to detect the generated

hydrogen.

2.4. Morphology characterization

Sample morphology analysis and elemental analysis were conducted using a JEOL-2100F transmission electron microscope (TEM) with an acceleration voltage of 200 kV. The characterization method involved dropping the catalyst sample solution onto an ultrathin carbon film, thoroughly drying it, and then proceeding with the characterization process.

3. Results and discussion

3.1. Effect of reactant ratio on particle size

First, we investigated the influence of reactant ratios on the size of ZIF-8 nanoparticles. Since most of the existing literature synthesizes ZIF-8 under room temperature conditions, we chose 30 ℃ as the reaction temperature for subsequent examination of the temperature effect on particle size [8-10]. By conducting experiments with a molar ratio of zinc acetate to dimethylimidazole of 1:1 (Fig. 1(a-c)), we clearly observed that the synthesized ZIF-8 nanoparticles exhibited an uneven size distribution, with particles larger than 1 micron. In contrast, for experiments with a molar ratio of zinc acetate to dimethylimidazole of 1:4 (Fig. 1(d-f)), we found that the synthesized ZIF-8 particles showed a uniform size distribution, with an average particle size of around 1 micron. Further observing the results of experiments with a molar ratio of zinc acetate to dimethylimidazole of 1:8 (Fig. 1(g-i)), we noticed that although the obtained ZIF-8 nanoparticles exhibited an uneven size distribution, the average particle size was smaller, roughly ranging from 200 nanometers to 1 micron.

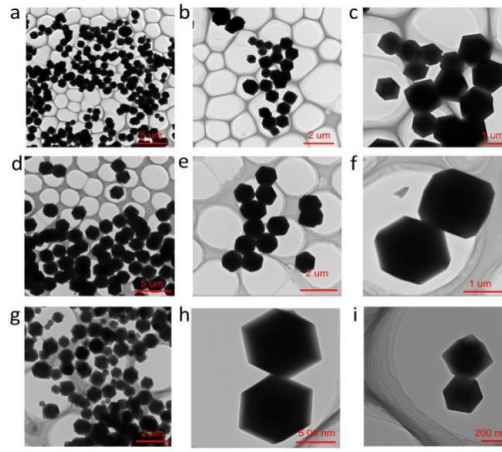

Fig. 1. Transmission electron microscope (TEM) images of ZIF-8 prepared with different molar ratios of zinc acetate and dimethylimidazole. Specifically, images a-c correspond to a molar ratio of 1:1; images d-f correspond to a molar ratio of 1:4; and images g-i correspond to a molar ratio of 1:8

These results indicate that reactant ratios have a significant impact on the particle size during ZIF-8 synthesis. When the molar ratio of zinc acetate to dimethylimidazole is 1:4, the resulting ZIF-8 nanoparticles exhibit a more uniform size distribution, which might be attributed to the fact that in this ratio, the stoichiometry of reactants is closer to the ideal conditions for structural formation, thereby promoting uniform crystal growth. On the other hand, when the molar ratio of reactants increases to 1:8, even though the particle size distribution remains uneven, the average particle size decreases. This phenomenon could be attributed to the excess dimethylimidazole acting as a dispersant during the reaction, hindering the aggregation process of particles [11]. After

examining the influence of reactant ratios, the next step will involve investigating the effect of temperature on ZIF-8 particle size.

3.2. Effect of inverse temperature on particle size

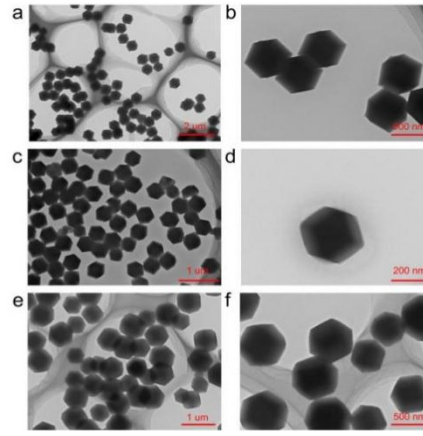

Fig. 2. Transmission electron microscope (TEM) images of ZIF-8 synthesized at different reaction temperatures. Specifically, images a and b correspond to a reaction temperature of 40 ℃; images c and d correspond to 50 ℃; and images e and f correspond to 60 ℃

After thoroughly exploring reactant ratios, we found that ZIF-8 particles synthesized with a molar ratio of zinc acetate to dimethylimidazole of 1:4 exhibited a relatively uniform size distribution. Building on this result, we selected this ratio condition to further investigate the effect of different reaction temperatures on the synthesized ZIF-8 particles.

Firstly, images in Fig. 2(a) and b correspond to experimental conditions with a reaction temperature of 40 ℃. Under this condition, the synthesized ZIF-8 particles were observed to have a uniform size distribution of approximately 500 nanometers. Subsequently, images in Fig. 2(c) and d display ZIF-8 particles synthesized at a reaction temperature of 50 ℃. Similarly, the particle size of the synthesized product also maintained a relatively uniform distribution, around 200 nanometers. Further, ZIF-8 particles synthesized at a reaction temperature of 60 ℃, as shown in images e and f in Fig. 2, also exhibited a uniform size distribution of around 500 nanometers. Compared to the uniform particle size of approximately 1 micron synthesized under the previously mentioned 30 ℃ condition, it's evident that particle sizes vary under different temperature conditions.

Notably, the trend of particle size variation at different temperatures displays a clear pattern. As the temperature gradually increased from 30 ℃ to 60 ℃, the size of synthesized ZIF-8 particles first decreased and then increased. This phenomenon can be attributed to changes in crystal nucleation and growth rates at different temperature conditions, resulting in the alteration of particle sizes. Within the temperature range of 30 °C to 50 °C, the increased crystal nucleation rate played a dominant role, leading to a reduction in particle size. However, as the temperature continued to rise, the crystal growth rate took precedence, resulting in an increase in particle size [12-13].

From the above results, it's evident that reaction temperature significantly impacts the size of ZIF-8 synthesized particles. By adjusting the reaction temperature, we successfully achieved the preparation of ZIF-8 nanoparticles with different sizes: 200 nanometers, 500 nanometers, and 1 micron. This provides an ideal sample set for investigating the effect of particle size on photocatalytic hydrogen production performance in subsequent research.

3.3. Photocatalytic hydrogen production of ZIF-8 with different particle sizes

Further experimental results revealed significant differences in the photocatalytic hydrogen production performance of ZIF-8 at different sizes. Specifically, ZIF-8 nanoparticles with sizes of 200 nanometers, 500 nanometers, and 1 micron exhibited hydrogen production rates of 8.1, 18.3, and 10.3 $\mu mol \cdot g^{-1} \cdot h^{-1}$, respectively. This trend demonstrates the clear influence of ZIF-8 particle size on its photocatalytic hydrogen production performance. Notably, as particle size increased, the photocatalytic performance initially increased and then decreased. This phenomenon might be closely related to the pore size of MOF materials.

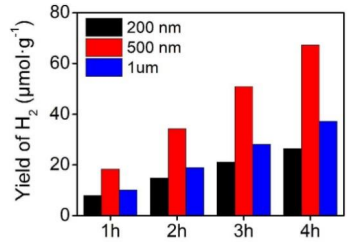

Fig. 3. Photocatalytic hydrogen production of ZIF-8 with different particle sizes

During the photocatalytic process, an appropriately sized pore can provide a better catalytic reaction interface and higher catalytic activity. Thus, an increase in particle size could lead to excessively large pore sizes, resulting in reduced photocatalytic hydrogen production performance. However, the outstanding photocatalytic performance of ZIF-8 particles with a size of 500 nanometers might be attributed to their pore size being well-suited to the requirements of the photocatalytic hydrogen production reaction. In summary, our research provides robust experimental groundwork for the application of ZIF-8 in the field of photocatalytic hydrogen production. By modulating the particle size of ZIF-8, we can attain various photocatalytic performances, offering important insights for further optimizing photocatalytic hydrogen production materials and exploring their mechanisms. With a deeper understanding of MOF material properties, the prospects for the application of materials like ZIF-8 in clean energy conversion will become even more promising.

4. Conclusions

Based on the comprehensive experimental results discussed above, the following conclusions can be drawn. Firstly, through the investigation of the influence of reactant ratios on the size of ZIF-8 nanoparticles, it is evident that reactant ratios play a significant regulatory role in the synthesis of ZIF-8 particles. When the molar ratio of zinc acetate to dimethylimidazole is 1:4, the synthesized ZIF-8 particles exhibit a uniform size distribution. This may be attributed to the fact that this ratio results in a closer approximation to the ideal conditions for structural formation, facilitating uniform crystal growth. Secondly, we explored the impact of reaction temperature on the size of ZIF-8 nanoparticles. The results indicate that under different temperature conditions, the size of synthesized ZIF-8 particles undergoes changes, with size decreasing initially and then increasing as temperature rises. This phenomenon, related to changes in crystal nucleation and growth rates, further highlights the significance of reaction temperature in ZIF-8 synthesis.

Regarding photocatalytic hydrogen production performance, we investigated the performance of ZIF-8 nanoparticles of different sizes in photocatalytic hydrogen production reactions. The results reveal that ZIF-8 nanoparticles with sizes of 200 nanometers, 500 nanometers, and 1 micron exhibit hydrogen production rates of 8.1, 18.3, and 10.3 $\mu mol \cdot g^{-1} \cdot h^{-1}$, respectively. This trend demonstrates the notable impact of ZIF-8 particle size on its photocatalytic hydrogen production performance, with an optimal particle size that maximizes photocatalytic performance.

This could be closely related to pore size, where an appropriate pore size can provide better catalytic activity. Among ZIF-8 particles of different sizes, ZIF-8 particles with a size of 500 nanometers exhibit superior photocatalytic hydrogen production performance, likely due to their pore size being more compatible with the requirements of the photocatalytic reaction.

These findings unveil a novel approach to optimizing photocatalytic hydrogen production materials, presenting groundbreaking insights into the potential of MOF materials like ZIF-8 in energy conversion. By advancing our understanding of these material properties, we underscore the pioneering role such materials could play in the forefront of clean energy solutions.

Acknowledgements

The authors have not disclosed any funding.

Data availability

The datasets generated during and/or analyzed during the current study are available from the corresponding author on reasonable request.

Conflict of interest

The authors declare that they have no conflict of interest.

References

[1] W. Zhang, Y. Huang, J. Shao, and H. Wu, "Research progress of semiconductor nanophotocatalyst," *Development and Application of Materials*, Vol. 27, No. 3, pp. 92–96, 2012, https://doi.org/10.19515/j.cnki.1003-1545.2012.03.021

[2] M. Y. Masoomi, A. Morsali, A. Dhakshinamoorthy, and H. Garcia, "Mixed-metal MOFs: unique opportunities in metal-organic framework (MOF) functionality and design," *Angewandte Chemie*, Vol. 131, No. 43, pp. 15330–15347, Oct. 2019, https://doi.org/10.1002/ange.201902229

[3] Y. Gu, Y.N. Wu, L. Li, W. Chen, F. Li, and S. Kitagawa, "Controllable modular growth of hierarchical MOF-on-MOF architectures," *Angewandte Chemie*, Vol. 129, No. 49, pp. 15864–15868, Dec. 2017, https://doi.org/10.1002/ange.201709738

[4] F. He et al., "ZIF-8 derived carbon (C-ZIF) as a bifunctional electron acceptor and HER cocatalyst for g-C3N4: construction of a metal-free, all carbon-based photocatalytic system for efficient hydrogen evolution," *Journal of Materials Chemistry A*, Vol. 4, No. 10, pp. 3822–3827, 2016, https://doi.org/10.1039/c6ta00497k

[5] F. Fu et al., "Highly selective and sharp volcano-type synergistic Ni_2Pt@ZIF-8-catalyzed hydrogen evolution from ammonia borane hydrolysis," *Journal of the American Chemical Society*, Vol. 140, No. 31, pp. 10034–10042, Aug. 2018, https://doi.org/10.1021/jacs.8b06511

[6] S. Feng et al., "Modifying $CsPbX_3$ (X = Cl, Br, I) with a zeolitic imidazolate framework through mechanical milling for aqueous photocatalytic H_2 evolution," *ACS Applied Energy Materials*, Vol. 5, No. 5, pp. 6248–6255, May 2022, https://doi.org/10.1021/acsaem.2c00615

[7] M. Zhang, Q. Shang, Y. Wan, Q. Cheng, G. Liao, and Z. Pan, "Self-template synthesis of double-shell TiO2@ZIF-8 hollow nanospheres via sonocrystallization with enhanced photocatalytic activities in hydrogen generation," *Applied Catalysis B: Environmental*, Vol. 241, pp. 149–158, Feb. 2019, https://doi.org/10.1016/j.apcatb.2018.09.036

[8] Z. Liu et al., "Construction of single Ni atom-immobilized ZIF-8 with ordered hierarchical pore structures for selective CO_2 photoreduction," *ACS Catalysis*, Vol. 13, No. 10, pp. 6630–6640, May 2023, https://doi.org/10.1021/acscatal.3c01118

[9] B. Yan, Z. Sun, Y. Han, H. Meng, and X. Zhang, "Tightly contacted heterojunction of ZnS/ZIS/In2S3: In situ construction from ZIF-8@MIL-68(In) and visible-light induced photocatalytic hydrogen generation," *Separation and Purification Technology*, Vol. 320, p. 124193, Sep. 2023, https://doi.org/10.1016/j.seppur.2023.124193

[10] N. Kang et al., "Dramatic acceleration by visible light and mechanism of AuPd@ZIF-8-catalyzed ammonia borane methanolysis for efficient hydrogen production," *Journal of Materials Chemistry A*, Vol. 11, No. 10, pp. 5245–5256, Mar. 2023, https://doi.org/10.1039/d2ta08396e

[11] S. Sun, H. Yu, M. Hua, L. Zhang, C. Gao, and X. Cheng, "Engineering ZIF-8 modified NaNbO3 perovskite photocatalyst toward high efficiency photocatalysis based on piezo-phototronic effect," *Catalysis Communications*, Vol. 181, p. 106713, Aug. 2023, https://doi.org/10.1016/j.catcom.2023.106713

[12] P. Behera, A. Ray, S. P. Tripathy, L. Acharya, S. Subudhi, and K. Parida, "ZIF-8 derived porous C, N co-doped ZnO modified B-g-C3N4: A Z-Scheme charge dynamics approach operative towards photocatalytic hydrogen evolution and ciprofloxacin degradation," *Journal of Photochemistry and Photobiology A: Chemistry*, Vol. 436, p. 114415, Mar. 2023, https://doi.org/10.1016/j.jphotochem.2022.114415

[13] M. Chen, H. Fang, C. Wang, J. Xu, and L. Wang, "Enhanced photocatalytic Cr(VI) reduction and H2 production of CdSe quantum dots supported on Co-encapsulated N-doped carbon," *Journal of the Taiwan Institute of Chemical Engineers*, Vol. 146, p. 104798, May 2023, https://doi.org/10.1016/j.jtice.2023.104798